Journal of Optoelectronics and Advanced Materials Vol. 7, No. 2, April, p. 933 - 950

Review Paper

TEMPERATURE DISTRIBUTION IN D. C. JOULE-HEATED AMORPHOUS MAGNETIC MATERIALS

I. Aştefănoaei*, D. Radu, H. Chiriac[a]

"Al.I. Cuza" University, Faculty of Physics, Carol I Blvd., No. 11,
RO-700050, Iasi, Romania
[a]National Institute of Research and Development for Technical Physics, 47 Mangeron Blvd., Iasi 3, Romania

The purpose of this paper is to present an improved theoretical and numerical model for the calculation of the temperature distribution in the amorphous magnetic materials such as: ribbons, conventional wires and glass-covered microwires, passed by an electrical direct current (d.c.) taking into account the d.c. Joule heating effects (conduction, convection and radiative heat losses and the structural changes appeared during the crystallization process of the conventional amorphous wires). The process of sample heating is accurately described by this improved theoretical model. The calculated temperature values are experimentally verified through magnetic measurements using a fluxmeter method performed on amorphous ribbons, conventional wires and respectively, glass-covered microwires with known Curie temperature. The theoretical results are in very good agreement with the experimental ones.

(Received October 12, 2004; accepted March 23, 2005)

Keywords: Amorphous magnetic materials, Glass-covered microwires, Amorphous ribbons and wires

1. Introduction

Joule heating has proven to be a rather powerful tool to achieve fast structural and/or compositional changes in magnetic materials such as amorphous ribbons, conventional amorphous wires and respectively, amorphous glass-covered microwires (AGCM). Many comprehensive works have been published in the early '90 (*e.g.* [1, 2, 3, 4]), indicating advantages and disadvantages of this method. Anyway, the search for improved physical properties in metastable systems (such as the ones examined in this paper) is still going on, so that any real improvement or new approach is still useful and of great interest.

Magnetic materials prepared by rapid quenching from the melt as wires or ribbons present a special interest for basic research and for technological applications [5]. It is well known [6] that thermal treatments can improve and stabilize the physical properties of amorphous materials produced by rapid solidification techniques. Theoretical and experimental results suggest that some other properties related to the structure of the material may be controlled and favorably modified by application of a suitable thermal treatment [7].

Direct current (d.c.) Joule heating techniques have always been of great help in the researches on thermal annealing of the magnetic amorphous materials. These techniques allow us to observe the structural transformations that occur in the material by effect of the treatment itself. This annealing method is based on the thermal effect of the electrical d.c. which passes through an amorphous sample [8]. One of the difficult problems concerning these treatments is to know the value of temperature corresponding to a given annealing electrical d.c., that passes through the

* Corresponding author: iordana@uaic.ro

sample. The use of d. c. Joule heating, in order to change the sample's properties, implies the knowledge of the sample's temperature as a function of the applied d.c. $I(A)$.

The aim of this paper is to present an improved theoretical model for the calculation of the temperature distribution in an amorphous sample passed by an electrical d.c. and to compare our theoretical results with the experimental data. We will determine the temperature in both steady and transient states, considering that the energy developed by Joule effect is consumed for the increase of the internal energy of the sample (in the transient state) and for the compensation of the radiation and convection heat losses (in the steady state). We have explicitly taken into account the presence of convective dissipation. This is an improvement with respect to older models because the convection cannot be completely ruled out by vacuum techniques.

As it is very well known, an electrical resistivity variation leads to a variation of the developed Joule power, and, subsequently, to a corresponding variation in the temperature distribution. For this reason, we must consider at least a linear dependence of the resistivity on temperature. In the amorphous materials, electrical resistivity always exhibits reversible and irreversible changes on heating; even low-temperature annealing may lead to some change upon coming back to room temperature. Moreover, Joule heating is specifically exploited to induce structural changes (including relaxation of the amorphous phase or nanocrystallization, when applicable). These changes may give rise to resistivity changes much higher than the simple linear temperature dependence. Nevertheless, we emphasize that in the present theoretical model, for ribbons and glass-covered microwires we have not considered the changes which can appear in the electrical resistivity as a result of the sample's crystallization. The effect of these changes becomes significant only for those values of the direct current that lead to temperatures over the crystallization ones, namely to temperatures higher than those used for heat treatments in order to improve the magnetic properties of the amorphous materials. However, for Joule-heated amorphous $Fe_{77.5}B_{15}Si_{7.5}$ wires we have also analyzed the crystallization mechanism in the non-isothermal process in terms of the kinetics transformations for the solid-state phase transformations. More precisely, in this case we have developed a numerical model within the context of the classical theory of phase evolution applied to conventional amorphous wires to simulate the kinetics of nucleation during the non-isothermal crystallization process.

2. Steady state and transient temperature distribution in d. c. Joule-heated amorphous materials

In this section we calculate the temporal and radial distribution of the temperature, in the transient and steady states for the amorphous stages of the samples (that means, for those values of the electrical d.c. that lead to the temperatures situated below the one corresponding to the onset of the crystallization process). The linear dependence of the electrical resistivity on the temperature was also taken into account.

To determine the temperature distribution in the amorphous samples annealed by Joule effect, we will use the Fourier heat conduction equation [9] with the corresponding boundary conditions.

Let's consider an amorphous sample (a ribbon, a conventional wire or an AGCM), placed in "vacuum" at a pressure less than $1\,Pa$, passed by an electrical d.c.. We associate a Cartesian system of coordinates (x, y, z) to the ribbon, having the Oz – axis along the ribbon's length, Ox – axis along the ribbon's width and Oy – axis along the ribbon's thickness. For wires (with- and without glass insulation) we associate a cylindrical system of coordinates (r, θ, z) to the sample having the Oz – axis along the wire's axis and we assume that the heat loss by Thomson effect is negligible (the ends of the samples are thermally isolated). The cylindrical metallic core of the amorphous glass-covered microwire has the radius R_1, and the glass insulation has the thickness $R_2 - R_1$, where R_2 is the total microwire's radius (metal + glass).

The heat developed in the unit volume by Joule effect has the form

$$W_i = \rho\, j^2(sc) = \rho_0 \left\{1 + \alpha\left[T(sc, t) - T_0\right]\right\} j^2(sc), \tag{1}$$

where $\rho = \rho(sc, t)$ is the resistivity at the temperature $T(sc, t)$, being given by the well known relation,

$$\rho(sc,\ t) = \rho_0 \left\{1 + \alpha\left[T(sc,t) - T_0\right]\right\}. \tag{2}$$

Here α is the thermal coefficient of the resistivity, t is the time during which the electrical dc passes through the sample, ρ_0 is the resistivity at the room temperature T_0, and $j(sc)$ is the current density distribution in the sample. The "sc" variable in the above functions means "spatial coordinates": for the ribbon the "sc" variable shall be replaced by the both spatial coordinates x and y, while for the wires (with- and without glass insulation) by the radial coordinate r. Also, in the case of the amorphous glass-covered microwire, the considerations that we develop in this section are valid only for the metallic core of the microwire.

Concerning the variation of the current density j as a function of "sc", we must point out that, because of the small dimensions of the sample (the experimental samples have a cross-section of $\left(10^{-12} \div 10^{-8}\right) m^2$), the spatial variations of the electrical field in the samples can be neglected. Because of that, if we take a constant value for the current density, then, we will introduce a maximum relative error on j, given by

$$\left|\delta j\right| = \left[1 - \beta + (\alpha T^*)^{-1}\right]^{-1}\left[\delta T + (1-\beta)\delta\alpha\right], \tag{3}$$

which, for the ribbon has the numerical value 0.012, whereas for the wires this numerical value is 0.0052. In the above equation $\beta = T_0 / T^*$, with $T^* \equiv T(0)$. The significance of $T(sc)$ is given as follows, while δT and $\delta\alpha$ are, respectively, the relative errors on temperature and thermal coefficient of the resistivity. Thus, taking into account (3), we may consider with a corresponding level of confidence that $j(sc) \equiv j = I / S = const.$

The heat generated in the sample is a function of "sc" and the time t, for each value of the electrical d.c. $I(A)$. In the transient state the conservation law of energy for the sample becomes

$$\rho_M c\ \left(dT / dt\right) = \left(\rho_\infty - \rho\right) I^2 S^{-2}, \tag{4}$$

where ρ_M is the mass density, c is the specific heat and $\rho_\infty = \rho_\infty(sc)$ is the electrical resistivity in steady state. The temperature field $T(sc,\ t)$ can be obtained by integrating (4) and taking into account (2). The result is

$$T(sc,\ t) = T_0 + \left[T_\infty(sc) - T_0\right]\left[1 - \exp\left(-\alpha\rho_0 I^2 \rho_M^{-1} c^{-1} S_1^{-2}\ t\right)\right]. \tag{5}$$

Here $T_\infty(sc)$ is the temperature of the sample[2] in steady state (at the thermal equilibrium) and S_1 is the cross-section of the sample (for the ribbon $S_1 = gl$, g being the thickness of the ribbon and l – its width; for the conventional wire $S_1 = \pi R_0^{\ 2}$, R_0 being the radius of the wire, while for the amorphous glass-covered microwire $S_1 = \pi R_1^{\ 2}$ is the cross-section of the microwire's metallic core).

Using the Fourier heat conduction equation [9] and the expressions corresponding to the boundary conditions, let's calculate the equilibrium temperature, $T_\infty(sc)$. In steady state ($t \to \infty$), the thermal equilibrium between the sample and the environmental medium is achieved. In this case, the heat generated by Joule effect is lost by convection and radiation processes.

2.1 The Temperature Distribution in d. c. Joule-heated amorphous ribbons

The Fourier heat conduction equation,

$$\frac{\partial^2 T_\infty(x,\ y)}{\partial x^2} + \frac{\partial^2 T_\infty(x,\ y)}{\partial y^2} + \frac{W_i}{k} = 0, \tag{6}$$

with the initial conditions,

[2] In the case of the glass-covered microwire this is the metallic core's temperature.

$$T_\infty(x,\ y,\ I=0)\ =T_0,\quad \rho\left(x,\ y,\ I=0\right)=\rho_0 \tag{7}$$

has the general solution

$$T_\infty(x,\ y)=T_0-\alpha^{-1}+C(I)\cosh(my)\cos\left(x\sqrt{m^2+\alpha\rho_0 I^2k^{-1}S^{-2}}\right). \tag{8}$$

In the equation (8), k is the thermal conductivity and $m=m(I)$ is a function of the parameter $I(A)$ (the intensity of the electrical dc). For $I=0$, from (7) and (8) it follows that $m(0)=0$. Now, using the relation (2) and the general solution (8) we are able to find the electrical resistivity in the steady state, $\rho_\infty(x,\ y)$:

$$\rho_\infty(x,\ y)=\rho_0 C(I)\alpha\cosh(my)\cos\left(x\sqrt{m^2+\alpha\rho_0 I^2k^{-1}S^{-2}}\right). \tag{9}$$

For $I=0$, from the initial conditions (7) and (9) it results that

$$C(0)=1/\alpha. \tag{10}$$

In order to determine the temperature distribution in the ribbon, we must consider the corresponding boundary conditions. Thus, on the ribbon's surface, the energy conservation law can be written as follows

$$W_i V=Q_{conv}+Q_{rad}, \tag{11}$$

where V is the volume of the ribbon, Q_{conv} is the convective heat loss [9],

$$Q_{conv}=p\left[T_\infty(x,\ y)-T_0\right]A_1\sqrt{2R\left(\pi M T_\infty(x,\ y)\right)^{-1}}\ ,\ \text{for}\ x=\pm\tfrac{l}{2},\ y=\pm\tfrac{g}{2}, \tag{12}$$

and Q_{rad} is the radiative heat loss [9],

$$Q_{rad}=\sigma\varepsilon A_1\left[T_\infty^{\ 4}(x,\ y)-T_0^{\ 4}\right],\ \text{for}\ x=\pm\tfrac{l}{2},\ y=\pm\tfrac{g}{2}. \tag{13}$$

In the above two relations $A_1=2L(l+g)$ is the area of the surface through which the radiative and convective heat exchange takes place, L is the length of ribbon, σ is the Stefan-Boltzmann constant, R is the universal gas constant $R=8.31\ \ J/mol\cdot K$, p is the pressure $p=(101325/760)\times10^{-2}(N/m^2)$ and $M=29$ is the air molecular weight. We consider that the ribbon is subjected to an electrical d.c. Joule-heating treatment in vacuum at the pressure less than $1\ Pa$. As we already have stated, the thermal losses are attributable to both radiative and convective contributions. The second one can not be neglected because the vacuum state, technologically speaking, is not a perfect one. Thus, we will consider that on the surface of the ribbon $\left(x=\pm\tfrac{l}{2},\ y=\pm\tfrac{g}{2}\right)$, a fraction $s\ (0<s<1)$ from the radiative heat loss Q_{rad} represents the convective heat loss, Q_{conv},

$$Q_{conv}=sQ_{rad}. \tag{14}$$

In the most general case, the s ratio depends on the annealing electrical d.c., *i.e.* $s=s(I)$. It is very difficult to find out the ratio $s(I)$ either experimentally or explicitly (analytically). For this reason, the only way to determine this ratio is the numerical approach; in fact, as it will be shown we

don't need to know $s(I)$ explicitly, if we choose a proper handle of the boundary conditions. At the thermal equilibrium (in the steady state), the thermal energy developed in the unit volume by Joule effect is consumed in order to compensate the radiative and convective heat losses. Using the relations (11) and (14), for $x = \pm\frac{l}{2}$, $y = \pm\frac{g}{2}$ we obtained the following conditions:

$$W_\infty V = (s+1)Q_{rad} \ , \quad W_\infty V = \left(s^{-1}+1\right)Q_{conv} \ , \tag{15}$$

where, in agreement with (1), W_∞ is given by $W_\infty = \rho_\infty I^2 / S^2$. For the characteristics of the amorphous ribbon given in Table 1 we have found the numerical values of $C(I)$ for eight given values of electrical d.c., $I \in [0.1 \div 0.8] A$. Using these values we have calculated the numerical values of $m = m(I)$ and $s = s(I)$ (Table 2). As one can observe, the higher the value of the electrical d. c., the faster the equilibrium value of the temperature is reached. Besides, the higher the value of the electrical d.c., $I(A)$, the smaller the convective heat loss becomes because, according to (14), for increasing values of the electrical d.c. $I(A)$ there is a decreasing of the $s = s(I)$ coefficient.

Table 1. The characteristics of the amorphous sample.

Characteristic quantity	Significance	Value and measurement units
c	the specific heat	530 $J/kg\ K$
ε	the coefficient of the thermal emittance	0.43
k	the thermal conductibility	30 W/mK
k_1	the thermal conductibility of the metallic core	30 W/mK
k_2	the thermal conductibility of the glass insulation	1.177 W/mK
ρ_M	the mass density	7.2×10^3 kg/m^3
ρ_0	the resistivity at the room temperature	1.24×10^{-6} $\Omega\cdot m$
T_0	the room temperature	293 K
L	the length of the sample	250 mm
l	the width of the ribbon	1 mm
g	the thickness of the ribbon	30 μm
R_0	the radius of the conventional wire	60 μm
R_1	the radius of the metallic core	9 μm
R_2	the radius of the amorphous glass-covered microwire	18 μm

Table 2. The numerical calculated values of $m(I)$, and $s(I)$ for different values of electrical d.c. $I(A)$.

No.	$I = I(A)$	$m = m(I)$	$s = s(I)$
1	0.1	127.281	0.309
2	0.2	140.720	0.176
3	0.3	127.755	0.108
4	0.4	112.309	0.072
5	0.5	97.253	0.052
6	0.6	82.121	0.040
7	0.7	65.592	0.031
8	0.8	44.810	0.025

The spatio-temporal distribution of the temperature $T(x,\ y,\ t)$ in the Joule-heated ribbons is

$$T_i(x,\ y,\ t)=T_0+\left[C_i(I)\cosh(my)\cos\left(x\sqrt{m^2+\alpha\rho_0 I^2k^{-1}S^{-2}}\right)-\alpha^{-1}\right]\left[1-\exp\left(-\alpha\rho_0 I^2\rho_M^{-1}c^{-1}S^{-2}\ t\right)\right],\quad \left(i=\overline{1,\ 8}\right). \tag{20}$$

while the spatial distribution of the temperature $T_\infty(x,\ y)$ in the steady state ($t\to\infty$) is

$$\left[T_\infty(x,\ y)\right]_i=T_0-1/\alpha+C_i(I)\cosh(my)\cos\left(x\sqrt{m^2+\alpha\rho_0 I^2/kS^2}\right),\quad \left(i=\overline{1,\ 8}\right). \tag{21}$$

As one observes from relation (20), the higher the value of the direct current, the faster the equilibrium value of the temperature is reached. We have also obtained the electrical resistivity of the ribbon in the transient state by taking into account the relations (2) and (20),

$$\rho\left(x,\ y,\ t\right)=\rho_0+\rho_0\left[C(I)\alpha\cosh(my)\cos\left(x\sqrt{m^2+\alpha\rho_0 I^2k^{-1}S^{-2}}\right)-1\right]\left[1-\exp\left(-\alpha\rho_0 I^2\rho_M^{-1}c^{-1}S^{-2}\ t\right)\right].$$

2.2 The temperature distribution in d. c. Joule-heated amorphous conventional wires

In the steady state, the thermal equilibrium of a conventional wire is described by general solution of the Fourier heat conduction equation [9],

$$\frac{1}{r}\frac{d}{dr}\left(r\frac{dT_\infty(r)}{dr}\right)+\frac{W_i}{k}=0, \tag{22}$$

and the initial conditions,

$$T(r,\ I=0)=T_0,\quad \rho\left(r,\ I=0\right)=\rho_0\quad . \tag{23}$$

The general solution of the equation (22) is

$$T_\infty(r)=T_0-\alpha^{-1}+C(I)J_0\left(r\sqrt{\alpha\rho_0 I^2k^{-1}S^{-2}}\right) \tag{24}$$

where the integration "constant" $C=C(I)$, is a function of the same parameter $I(A)$ (the intensity of the electrical d.c.) while k is the thermal conductivity. For $I=0$, from (23) and (24) we get $C(0)=1/\alpha$.

After a straightforward calculation, from (2) and (24) we find the electrical resistivity in the steady state, $\rho_\infty(r)$:

$$\rho_\infty(r)=\rho_0C(I)\alpha J_0\left(r\sqrt{\alpha\rho_0 I^2k^{-1}S^{-2}}\right). \tag{25}$$

In the following, we consider the corresponding boundary conditions to determine the temperature distribution in the conventional wire. Thus, the energy conservation law on the microwire's surface can be written as

$$W_iV=Q_{conv}+Q_{rad}, \tag{26}$$

where V is the volume of the sample, Q_{conv} is the convection heat loss [9]:

$$Q_{conv}=p\left[T_\infty(r)-T_0\right]A_1\sqrt{2R\left(\pi MT_\infty(r)\right)^{-1}}\ \text{, for } r=R_0, \tag{27}$$

and Q_{rad} is the radiative heat loss [9]

$$Q_{rad} = \sigma\varepsilon A_1\left[T_\infty^{\,4}(r) - T_0^{\,4}\right], \text{ for } r = R_0 . \tag{28}$$

In the above two relations $A_1 = 2\pi R_0 L$ is the area of the surface through which the radiative and convective heat exchange takes place. As in the ribbon's case, on the surface of the microwire, $r = R_0$, besides the radiative thermal loss, Q_{rad}, a fraction s $(0 < s < 1)$ from this radiative heat loss represents the convective heat loss, Q_{conv},

$$Q_{conv} = sQ_{rad} . \tag{29}$$

where s ratio can depend on the annealing d.c., *i.e.* $s = s(I)$. Using relations (26) and (29) for $r = R_0$, we obtained the following conditions:

$$W_\infty V = (s+1)Q_{rad} \;, \quad W_\infty V = \left(1/s+1\right)Q_{conv} , \tag{30}$$

where, in agreement with (1), W_∞ is given by $W_\infty = \rho_\infty I^2 / S^2$. The relations (30) lead us to

$$\left[\rho_0 C(I)\alpha I^2 J_0\left(R_0\sqrt{\alpha\rho_0 I^2 k^{-1}S^{-2}}\right)\left[2\sigma\varepsilon\pi^2 R_0^{\,3}(s+1)\right]^{-1} + T_0^4\right]^{1/4} = T_0 - \alpha^{-1} + C(I)J_0\left(R_0\sqrt{\alpha\rho_0 I^2 k^{-1}S^{-2}}\right) \tag{31}$$

and

$$\begin{aligned}\rho_0 C(I)\alpha I^2\left(2\pi^2 R_0^3\right)^{-1} J_0\left(R_0\sqrt{\alpha\rho_0 I^2 k^{-1}S^{-2}}\right) &= \left[C(I)J_0\left(R_0\sqrt{\alpha\rho_0 I^2 k^{-1}S^{-2}}\right) - \alpha^{-1}\right] \times \\ &\times\left(1+s^{-1}\right)p\sqrt{2R}\left\{\pi M\left[T_0 - \alpha^{-1} + C(I)J_0\left(R_0\sqrt{\alpha\rho_0 I^2 k^{-1}S^{-2}}\right)\right]\right\}^{-1/2} .\end{aligned} \tag{32}$$

For the characteristics of the amorphous conventional wire given by the Table 1 we find the numerical values for $C(I)$ and $s(I)$ as numerical solutions of transcendent equations (31) and (32), for ten given values of electrical d.c., $I \in [0.001 \div 0.5]A$ (Table 3).

Table 3. The numerical values of the $C(I)$, and $s(I)$ for different values of electrical d.c. $I(A)$.

No.	$I = I(A)$	$C = C(I)$	$s = s(I)$
1	0.0010	5714.39	0.6230
2	0.0015	5714.52	0.6336
3	0.0020	5714.70	0.6491
4	0.0025	5714.92	0.6699
5	0.0030	5715.18	0.6968
6	0.0035	5715.48	0.7309
7	0.0040	5715.81	0.7737
8	0.0045	5716.15	0.8273
9	0.0050	5716.50	0.8949
10	0.0055	5716.85	0.9807

The radial and temporal distribution of the temperature $T(r, t)$ in the Joule-heated conventional wires results by replacing the numerical values given in Table 3 in the general expression (5). The result is:

$$T_i(r,\ t)=T_0+\left[C_i(I)J_0\left(r\ \sqrt{\alpha\rho_0 I^2k^{-1}S^{-2}}\right)-\alpha^{-1}\right]\left\{1-\exp\left[-\alpha\rho_0 I^2\left(\rho_M cS^2\right)^{-1}t\right]\right\},\quad \left(i=\overline{1,\ 10}\right),\qquad (33)$$

while the radial distribution of the temperature $T_\infty(r)$ at the thermal equilibrium (the steady state, $t\to\infty$) is

$$\left[T_\infty(r)\right]_i=T_0-1/\alpha+C_i(I)J_0\left(r\sqrt{\alpha\rho_0 I^2k^{-1}S^{-2}}\right),\quad \left(i=\overline{1,\ 10}\right).\qquad (34)$$

From (2) and (5) we obtain the electrical resistivity of the conventional wire in the transient state,

$$\rho\left(r,\ t\right)=\rho_0+\rho_0\left[C(I)\alpha J_0\left(r\sqrt{\alpha\rho_0 I^2k^{-1}S^{-2}}\right)-1\right]\left[1-\exp\left(-\alpha\rho_0 I^2\rho_M^{-1}c^{-1}S^{-2}\ t\right)\right].$$

2.3 The temperature distribution in d. c. Joule-heated amorphous glass-covered microwires

Using the Fourier heat conduction equation,

$$\frac{1}{r}\frac{d}{dr}\left(r\frac{dT_m(r)}{dr}\right)+\frac{W_i}{k_1}=0,\qquad (35)$$

and the expressions corresponding to the initial conditions,

$$T_m(r,\ I=0)\ =T_0,\ \rho\left(r,\ I=0\right)=\rho_0,\qquad (36)$$

we obtain the radial temperature distribution $T_m(r)$ in the metallic core of the amorphous glass-covered microwire, at the thermal equilibrium (steady state, $t\to\infty$):

$$T_m(r)=T_0-\alpha^{-1}+C(I)J_0\left(r\sqrt{\alpha\rho_0 I^2k_1^{-1}S_1^{-2}}\right),\qquad (37)$$

where: J_0 are the zero-order Bessel functions, k_1 is the thermal conductivity of the metallic core and $C=C(I)$ is the integration constant that is a function of electrical d.c. $I(A)$. For $I=0$, from (36) and (37) follows that $C(0)=\alpha^{-1}$. The electrical resistivity in the steady state, $\rho_\infty(r)$ is given by the relation,

$$\rho_\infty(r)=\rho_0C(I)\alpha J_0\left(r\sqrt{\alpha\rho_0 I^2k^{-1}S^{-2}}\right).\qquad (38)$$

In order to determine the temperature distribution in the metallic core, the corresponding boundary conditions must be considered.

2.3.1. The temperature distribution in the glass insulation

In the steady state ($t\to\infty$), the thermal equilibrium between the sample and the environmental medium is achieved. In this case, the heat flux from the metallic core – generated by Joule effect – is received by the glass insulation. Using the Fourier heat conduction equation [9] for $R_1<r<R_2$,

$$\frac{1}{r}\frac{d}{dr}\left(r\frac{dT_g(r)}{dr}\right)=0,\qquad (39)$$

we shall calculate the equilibrium temperature of the glass insulation, $T_g(r)$. The general solution of equation (39) reads

$$T_g(r) = A_1 \ln r + A_2 , \tag{40}$$

where the integration "constants" $A_1 = A_1(I)$ and $A_2 = A_2(I)$ are functions of the same parameter $I(A)$, their physical significance being given in the following subsection.

2.3.2 Boundary conditions for the metal-glass interface

In order to determine the final expressions of the temperature $T_m(r)$ in the metallic core (37) and in the glass insulation (40), we must use the following boundary conditions:

i) In the thermal steady state, the heat flux from the metallic core is received by the glass insulation. This heat flux (from the metal-glass interface) must be continuous. So, for $r = R_1$ we must have

$$k_1 \left(dT_m / dr \right) = k_2 \left(dT_g / dr \right) , \tag{41}$$

where k_1 and k_2 are the coefficients of thermal conductivity of the amorphous metallic core and glass insulation, respectively;

ii) On the metal-glass interface ($r = R_1$), the temperatures from the adjacent regions must be equal,

$$T_m(R_1) = T_g(R_1) . \tag{42}$$

iii) In the steady state ($t \to \infty$), on the outer surface of the microwire, the thermal equilibrium between the sample and the environmental medium is achieved by the radiative heat loss:

$$-\left(dT_g / dr \right)\Big|_{r=R_2} = P k_2^{-1} \left[T^4(R_2) - T_0^4 \right], \tag{43}$$

where $P = \sigma \varepsilon 2L / R_2$ is the so-called *microwire's loss parameter*, L is the length of the sample. Using the boundary conditions given by (41), (42) and (43) we get the following expressions:

$$-k_1 k_2^{-1} R_1 C(I) J_1 \left(R_1 \sqrt{\alpha \rho_0 I^2 \left(k_1 \pi^2 R_1^4 \right)^{-1}} \right) \sqrt{\alpha \rho_0 I^2 \left(k_1 \pi^2 R_1^4 \right)^{-1}} = A_1 , \tag{44}$$

$$A_1 \ln R_1 + A_2 = T_0 - \alpha^{-1} + C(I) J_0 \left(R_1 \sqrt{\alpha \rho_0 I^2 \left(k_1 \pi^2 R_1^4 \right)^{-1}} \right) \tag{45}$$

and

$$A_1 \ln R_2 + A_2 = \left[T_0^4 - A_1 k_1 \left(R_2 P \right)^{-1} \right]^{1/4} , \tag{46}$$

where J_1 are the first-order Bessel functions. From (44), (45) and (46) we obtain the $C(I)$, $A_1 = A_1(I)$ and $A_2 = A_2(I)$ as follows:

The constant $A_1 = A_1(I)$ results as numerical solution of the following transcendent equation

$$A_1\left[\ln\left(\frac{R_1}{R_2}\right)+\frac{k_2 S_1}{R_1 I\sqrt{k_1\alpha\rho_0}}\frac{J_0\left(R_1\sqrt{\alpha\rho_0 I^2 k_1^{-1}\pi^{-2}R_1^{-4}}\right)}{J_1\left(R_1\sqrt{\alpha\rho_0 I^2 k_1^{-1}\pi^{-2}R_1^{-4}}\right)}\right]=T_0-\frac{1}{\alpha}-\left(T_0^4-\frac{A_1}{PR_2}\right)^{1/4}. \quad (47)$$

For each given value of the annealing current I (A), one obtains a corresponding numerical value of the "constant" $A_1 = A_1(I)$. Then, the numerical values of $C(I)$ simply results from

$$C(I)=-k_2 S_1\left(R_1 I\sqrt{k_1\alpha\rho_0}\right)^{-1}A_1\left[J_1\left(R_1\sqrt{\alpha\rho_0 I^2 k_1^{-1}\pi^{-2}R_1^{-4}}\right)\right]^{-1}, \quad (48)$$

where A_1 (already known) must be introduced. At the same time, the constant A_2 results immediately from (46). We observe that the parameter $C(I)$ depends on electrical d.c. $I = I(A)$, the material constants: α, ρ_0, k_1, k_2 and the sample's dimensions, R_1, R_2 and L. For different values of the electrical d.c $I(A)$, the structural changes (metastable phase relaxations) take place in the metallic region of the microwire. Due to this fact, the parameter $C(I)$ is called *the coefficient of metastable phase relaxations* and it explicitly contains the influences of the structural transformations that occur in the material by effect of the heat treatment itself.

For the amorphous glass-covered microwire's characteristics given by the Table 1 we have found the numerical values for $C(I)$, $A_1(I)$ and $A_2(I)$ as numerical solutions of nonlinear equations (46), (47) and (48), for eleven given values of electrical d.c. in the interval $I \in [1 \div 28]\ mA$ (Table 4). The higher the value of the direct current $I(A)$, the higher $C(I)$, $A_1(I)$ and $A_2(I)$ are.

Table 4. The numerical values of the $C = C(I)$, $A_1 = A_1(I)$ and $A_2 = A_2(I)$ for different values of electrical dc $I(A)$.

No.	$I(mA)$	$C(I)$	$A_1 = A_1(I)$	$A_2 = A_2(I)$
1	1	5772.63	- 0.001	58.3385
2	5	5845.17	- 0.018	130.681
3	7	5869.32	- 0.035	154.632
4	9	5890.25	- 0.058	175.293
5	14	5934.20	- 0.140	218.287
6	17.8	5962.61	- 0.229	245.668
7	21	5984.30	- 0.320	266.308
8	23	5997.06	- 0.383	278.309
9	25	6009.28	- 0.454	289.715
10	27	6021.05	- 0.530	300.588
11	28	6026.78	- 0.571	305.841

Introducing the numerical values of $C(I)$, $A_1(I)$ and $A_2(I)$ in the general relations (37), (5) and (40) we have obtained:

i) The spatial temperature distribution $T_m(r)$ in the steady state $(t \to \infty)$, at the thermal equilibrium in the microwire's metallic core,

$$T_m(r)=T_0-\alpha^{-1}+C(I)J_0\left(r\sqrt{\alpha\rho_0 I^2 k_1^{-1}S_1^{-2}}\right); \quad (49)$$

ii) The spatio-temporal distribution of the temperature, $T_m(r, t)$, in the Joule-heated amorphous glass-covered microwires, in the temperature region situated below the one corresponding to the onset of the crystallization process:

$$T_m(r,\ t) = T_0 + \left[C(I) J_0\left(rIS_1^{-1}\sqrt{\alpha\rho_0 k_1^{-1}} \right) - \alpha^{-1} \right] \left[1 - \exp\left(-\alpha\rho_0 I^2 \rho_M^{-1} c^{-1} S_1^{-2}\ t \right) \right]; \tag{50}$$

iii) The temperature distribution $T_g(r)$ in the steady state ($t \to \infty$) at the thermal equilibrium in the microwire's glass insulation,

$$T_g(r) = A_1(I) \ln r + A_2(I), \tag{51}$$

the transient temperature in the microwire's glass insulation being not relevant.

On the basis of the established relations (49), (50) and (51) with the numerical values of $C(I)$, $A_1(I)$ and $A_2(I)$ we have calculated the temporal evolution and radial distribution of the temperature at different values of the direct current that passes through an amorphous glass-covered microwire which has the composition $Fe_{77.5}Si_{7.5}B_{15}$ and the above mentioned characteristics. Taking into account the relations (2) and (5), we have obtained the electrical resistivity of the amorphous glass-covered microwire's metallic core in the transient state,

$$\rho_m(r,\ t) = \rho_0 + \rho_0 \left[C(I)\alpha J_0\left(r\ \sqrt{\alpha\rho_0 I^2 k^{-1} S_1^{-2}} \right) - 1 \right] \left[1 - \exp\left(-\alpha\rho_0 I^2 \rho_M^{-1} c^{-1} S_1^{-2}\ t \right) \right].$$

3. Thermal behavior and crystallization kinetics analysis of the amorphous conventional wires

In this section, our purpose is to analyze the crystallization mechanism in the non-isothermal process in terms of the kinetics transformations for the solid-state phase transformations in Joule-heated amorphous $Fe_{77.5}B_{15}Si_{7.5}$ wires. We present a numerical model which is able to describe the kinetics of non-isothermal crystallization process. In general, the transition from the amorphous phase to the crystalline phase is a complicated process. The crystallization process of the amorphous wires consists of two steps: nucleation and crystal growth. The nucleation can be described as a process in which molecules come into contact, orient and interact to form highly ordered structures, called nuclei. According to their environment, the crystals grow more or less regularly and exhibit different growth morphologies. Nucleation and crystal growth are not mutually exclusive: nucleation may take place while crystals grow on existing nuclei [10]. The most common approach used to describe the crystallization kinetics is the Johnson-Mehl-Avrami (JMA) model, in which the relative crystallinity varies as a function of time, $x = x(t)$. A very useful tool to understand and predict these phenomena is the numerical analysis method. In the following, we develop a numerical model within the context of the classical theory of phase evolution applied to amorphous conventional wires to simulate the kinetics of nucleation during the non-isothermal crystallization process. The aim of this study is to analyze the thermal behavior of the Joule-heated amorphous wires in such conditions. More precisely, we present a numerical model for the temporal evolution of the sample's temperature and for volume fraction crystallized with time, $x(t)$, assuming that the crystal growth and Avrami crystallization rate constant have an Arrhenius type temperature dependence $K = K[T]$. We also consider that the nucleation frequency K_0 is constant. The Avrami model [10] can be also used to analyze the non-isothermal crystallization process. In our model, the energy released during the crystallization process appears to be a function of temperature, rather than time, as in the case of isothermal crystallization, because the non-isothermal crystallization process may be considered to be composed of a great number of infinitesimally small isothermal crystallization steps. The crystallization rate parameter can be described by the exponential relation (Arrhenius form) $K[T] = K_0 \exp\left(-nQ/kT\right)$, where Q is the growth or diffusion activation energy, T is the absolute temperature and k is the Boltzmann constant. The activation energy Q is strongly dependent on the type of nucleation in the crystallization process.

From the direct experimental observations, it is known that the crystallization process in the Joule -heated amorphous wires is an exothermal one. In this case, the energy developed by the Joule effect is consumed in the crystallization process to increase the internal energy of the sample and to compensate the radiative heat losses. The increase of the applied d.c. $I(A)$ gives rise to an increase in the electrical resistivity and subsequently leads to the increase of internal energy. The final temperature of the sample results from the balance between the applied electrical power and dissipation effects in the fully crystallized sample. For a more accurate picture of the process, in our model, we consider the following working hypotheses:

- the structure dependent parameters like ρ_M and c are constant;
- the coefficient of the thermal emittance, ε, is constant during the heating treatment;
- the results obtained in the subsection 2.2, show that for different values of the applied d.c., the temperature of the sample is approximately constant in the whole cross-section of the conventional wire. For this reason in the following, we will neglect the conduction heat loss and we assume that the temperature in the sample's cross-section is constant.

In order to analyze the thermal behavior and crystallization process of the amorphous wires, we introduce a new time scale, whose zero is coincident with the onset of the crystallization process, at the steady-state temperature value of the heated amorphous sample, $T(r,I) \equiv T_M(I) = T_M$. The crystallization process of the sample starts from $t = 0$, when an additional amount of energy per unit time is homogeneously released to the sample. The crystallization power density, W_{ef} (expressed in W/m^3) is given by the expression

$$W_{ef}(t) = \Delta H_{eff}\left[dx(t)/dt\right], \tag{52}$$

where ΔH_{eff} is the amount of the total density of crystallization heat effectively contributing to the extra heating of the amorphous wire and relative crystallinity $x(t)$ represents the solution of the JMA's equation [11]. At the initial moment, $t = 0$, the transformed volume fraction is $x(0) = 0$, while at the equilibrium of the crystallinity phase, $t \to \infty$, $x(t \to \infty) = 1$. The rate of transformation $dx(t)/dt$ will be obtained in the following.

During the crystallization process of the sample, the energetic balance between the crystallization power density (52), the heat developed in the unit volume of the wire by Joule effect, $W_i = \rho(t)I^2/S^2$, and the radiative heat loss can be represented by the expression $\rho_M c\left[dT(t)/dt\right] = W_{ef}(t) + \rho(t)I^2/S^2 - P\left[T^4(t) - T_M^4\right]$, where

$$\rho(t) = \rho_{amorph}(t)x(t) + \rho_{crys}(t)\left[1 - x(t)\right] \tag{53}$$

is the electrical resistivity of the amorphous wire during the crystallization process. In this relation,

$$\rho_{amorph}(t) = \rho_{0m}\left\{1 + \alpha_{amorph}\left[T(t) - T_M\right]\right\} \tag{54}$$

represents the electrical resistivity of the amorphous phase, α_{amorph} is the corresponding thermal coefficient of this resistivity while

$$\rho_{crys}(t) = \rho_{0m}\left\{1 + \alpha_{crys}\left[T(t) - T_M\right]\right\} \tag{55}$$

represents the electrical resistivity of the crystalline phase, where α_{crys} is the corresponding thermal coefficient.

Thus, at the initial moment, $t = 0$, the electrical resistivity is $\rho(t=0) = \rho_{amorph}(t=0) = \rho_{0m}$, *i.e.*, the sample as a whole is in the amorphous state, while at the equilibrium of the crystalline phase,

$t \to \infty$, the electrical resistivity is given by $\rho(t \to \infty) = \rho_{crys}(t)$ (the sample is completely crystallized). Introducing the relations (54) and (55) in (53), we obtain the electrical resistivity $\rho(t)$ of the amorphous wire during the crystallization process

$$\rho(t) = \rho_{0m}\left\{1 + \alpha_{crys}\left[T(t) - T_M\right]\right\} + \rho_{0m}(\alpha_{amorph} - \alpha_{crys})\left[T(t) - T_M\right]x(t). \tag{56}$$

In the case of Joule heating, an increase of electrical resistivity implies a corresponding increase of the Joule power and subsequently a rapid increase of the wire's temperature. The kinetics of this process may be studied in order to precisely control the structural transformations of the amorphous wire during the crystallization process. The rate of transformation in the non-isothermal crystallization process [10], is given by the relation

$$dx(t)/dt = n\left[1 - x(t)\right]\left[-\ln[1 - x(t)]\right]^{(n-1)/n} K_0^{1/n} \exp\left(-Q/kT\right). \tag{57}$$

In the non-isothermal crystallization process of the sample, energetic balance between the crystallization power density (52), the heat developed in the unit volume by Joule effect in the sample, and radiative heat loss is given by

$$\begin{aligned}\rho_M c\left[dT(t)/dt\right] = \Delta H_{eff}\, n\left[1 - x(t)\right]\left[-\ln[1 - x(t)]\right]^{(n-1)/n} K_0^{1/n} \exp\left(-Q/kT\right) - \\ - P\left[T^4(t) - T_M^4\right] + \rho_{0m} I^2/S^2 + \rho_{0m}\left[\gamma x(t) + \alpha_{crys}\right]\left[T(t) - T_M\right] I^2/S^2,\end{aligned} \tag{58}$$

where $\gamma = \alpha_{amorph} - \alpha_{crys}$.

We consider the relations (57) and (58) as a differential equations system with the unknown quantities $T(t)$ and $x(t)$. Using the Runge-Kutta method for the differential equations system (Runge2D) in a Mathematica subroutine, we compute the solutions $T(t)$ and $x(t)$ with the initial conditions $T(t=0) = T_M$ and $x(t=0) = 0$, for the temporal evolution of the temperature and volume fraction crystallized with time in the non-isothermal crystallization kinetics analysis. Passing through the sample the same value of the electrical d.c., $I = 0.3\,A$, from the relations (33) and (34), we obtain the equilibrium temperature of the amorphous phase at the initial moment $T_M = 387.9\ ^\circ C$.

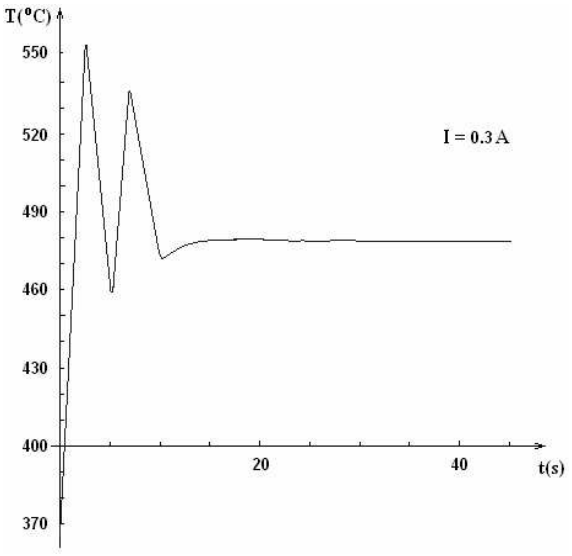

Fig. 1. The temporal evolution of the temperature $T(t)$ in the non-isothermal crystallization process.

By best fit to experimental data we consider the particular values for the adjustable parameters (the kinetic exponent $n = 3.6$ and $\Delta H_{eff} = 5.8 \cdot 10^8 J/m^3$). In our numerical analysis we will consider that in the non-isothermal crystallization process, the growth of diffusion activation energy is Q = 2.24 eV. Fig. 1 presents the numerical solution $T(t)$ of the differential equations system (57) and (58), i.e. the temperature of the sample $T(t)$ for the applied electrical dc $I = 0.3\,A$. We observe that the entire non-isothermal crystallization process predicted by this model is ranging from $T_M = 387.9\ ^\circ C$ to $T = 480\ ^\circ C$.

The numerical analysis gives for the temperature of the amorphous wire two relative maximum values, corresponding to successive stages of crystallization as follows: the first stage corresponds to the temperature $550\ ^\circ C$ and the second one to $539\ ^\circ C$. This behavior is in very good agreement with the experimental results obtained by differential scanning calorimetry (DSC) and presented in Fig. 2. This figure shows the dependence of the heat flow as a function of temperature (in $^\circ C$) for an conventional $Fe_{77.5}B_{15}Si_{7.5}$ wire. The DSC curve exhibits the two sharp peaks at $T_1 = 551\ ^\circ C$ and $T_2 = 543\ ^\circ C$. From Fig. 1 we deduce that the crystallization process in the considered amorphous wire, for a value of electrical dc $I = 0.3\,A$ starts at about $T_M = 387.9\ ^\circ C$ when $\rho_{0m} = 1.32 \times 10^{-6}\ \Omega \cdot m$.

Our model present a complete and synthetic description of the crystallization phenomena that occur in amorphous $Fe_{77.5}B_{15}Si_{7.5}$ wires. The thermo-numerical simulation gives a very good prediction, the obtained results being in very good agreement with the experimental measurements.

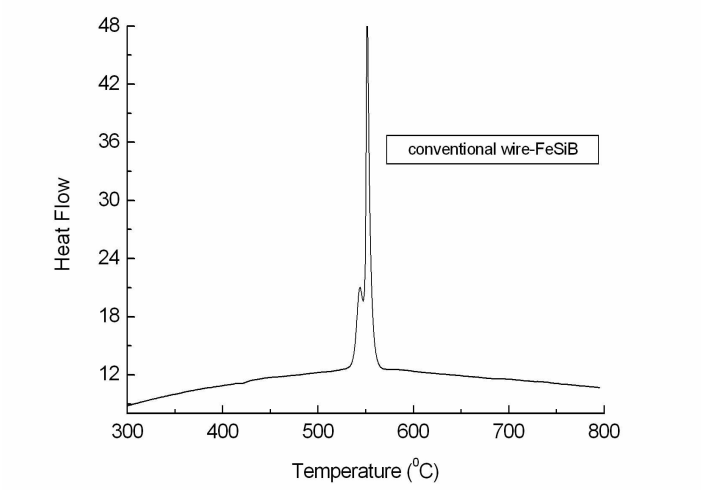

Fig. 2. The crystallization temperature from DSC.

4. Experimental results

Using the proposed theoretical model we can calculate the maximum values reached by the temperature in the samples for different values of the applied d.c. The utilization of d.c. Joule-heating technique in order to change the magnetic and electric samples' properties implies to know the temperature in the samples as a function of the applied d.c. value. Some experiments were made in order to measure the temperature in the samples by using a set of thermocouples or by using the infrared emission, but these procedures are complicated and – that is most important – can introduce huge experimental errors. We have experimentally verified the calculated values of the temperature in the samples for different values of the electrical d. c.. To this purpose we have measured (by a fluxmeter method) the magnetization value as a function of electrical d.c. that passes through the samples. The experimental set up is described in [8] and it consists of an evacuated sealed tube in which the samples are placed. This tube is introduced into a pick-up coil and then the whole ensemble is introduced into a magnetizing coil that produces a maximum measuring field of

$300\ A/m$. The voltage induced in the pick-up coil is integrated and amplified, being proportional with the samples' magnetization. The increase of the direct current that passes through the samples is generated by a programmable power supply which has a small enough increasing rate. By increasing the value of the electrical d.c. that passes through the samples, the magnetization decreases until it vanishes. The value of the electrical d. c. at which the magnetization becomes zero corresponds to the Curie temperature of the samples. For calibration we have used an amorphous $Fe_{77.5}B_{15}Si_{7.5}$ sample having $L = 1\ mm$. The calculated values are close enough to the experimentally estimated ones. Thus:

i) In the ribbon's case, for an electrical d. c. value of $I = 0.5\ A$ we have found

$$T^{calc} = 675.62\ K, \qquad T^{\exp} = 674\ K;$$

ii) In the microwire's case, for a d.c. value of $I = 0.07\ A$ we have obtained

$$T^{calc} = 367.62\ K, \quad T^{\exp} = 365\ K, \text{ while}$$

iii) In the glass-covered microwire's case, for a d.c. value of $I = 0.025\ A$ we have found

$$T_m^{\text{calc}} = 587.43\ K, \qquad T_m^{\exp} = 586\ K.$$

The small differences (the relative error on T^{calc} is $\delta T^{calc} = 0.24\ \%$ for the ribbon and glass-covered microwire and $\delta T^{calc} = 0.71\ \%$ for the microwire) could be attributed to the variation of the material's thermal constants, as well as to the effect of the structural changes which can appear in the heated samples, even at these temperatures. It is ascertained that the theoretical results are in very good agreement with the experiment. The process of sample heating is accurately described by this improved theoretical model, in which the thermal losses of radiative and convection nature have also been taken into account.

5. Results and discussions

Figs. 3, 4 and 5 present the temporal evolution of the temperature for the different values of the d.c. $I(A)$, for the three types of amorphous samples, namely: the ribbon, the conventional wire and, respectively, the glass-covered microwire. In these figures we observe an increase of temperature with the time during which the electrical d.c. passes through the samples, until it reaches the maximum equilibrium value. The higher the value of the direct current, the faster the maximum value of the temperature is reached.

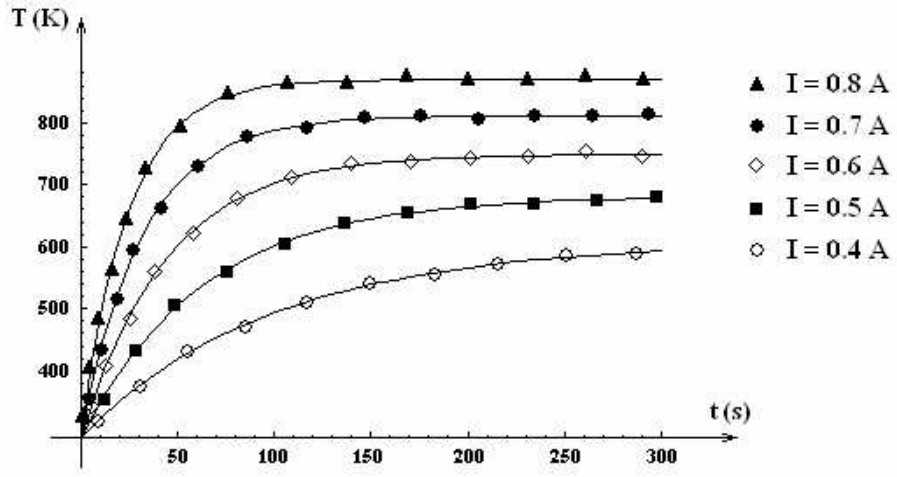

Fig. 3. The temporal evolution of the temperature $T(t)$ in the center of the ribbon.

Figs. 6, 7 and 8 illustrate the time dependence of the electrical resistivity for the different values of the applied dc in the same three cases, namely: the ribbon, the conventional wire and the glass-covered microwire.We observe that the electrical resistivity increases by increasing the value of the direct current. The shape of these curves is almost similar to that given in Figs. 3, 4 and 5 because we have considered a linear dependence of the samples' electrical resistivity on temperature.

Fig. 9 illustrates the tempera-ture distribution at the thermal equilibrium in the amorphous glass-covered microwire's cross-section for a value of the direct current of $I = 17.8\ mA$.

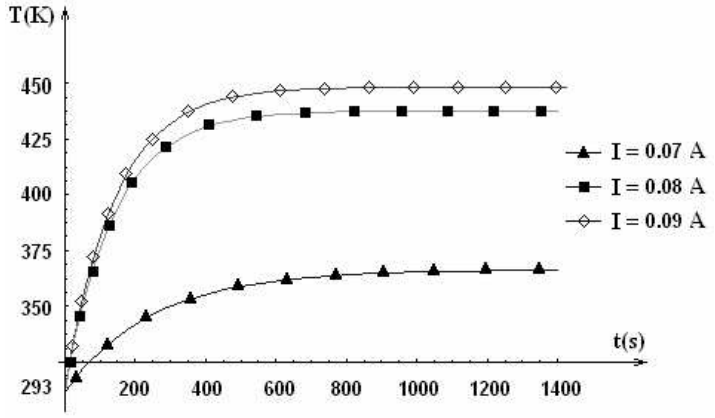

Fig. 4. The temporal evolution of the temperature $T(t)$ in center of the conventional wire.

As this figure shows, the temperature difference between the center of microwire's metallic core and its glass insulation is very small ($0.004\ ^{\circ}C$), and between its center and its outer glass surface is of $0.0163\ ^{\circ}C$. Thus, we can consider that the temperature is practically constant in the metallic core's cross section, in this way, the Joule effect annealing ensuring a uniform heating of sample. We observe an important decrease of the equilibrium temperature $T_g(r)$ in the microwire's glass insulation ($R_1 < r < R_2$) due to the radiative heat losses.

Fig. 10 shows the two theoretical curves that present the relationship between the annealing current I and temperature at the point $r = 1\ \mu m$ in the metallic region of the amorphous glass-covered microwire. There are small differences between these theoretical curves: the dotted line was obtained according to the theoretical model developed in [12], without considering the linear dependence of resistivity on temperature, but considering – by best fit to experimental data – the influence of the metastable phase relaxations through the coefficient $R(I)$, while the simple line is obtained by considering the theoretical results of improved theoretical model.

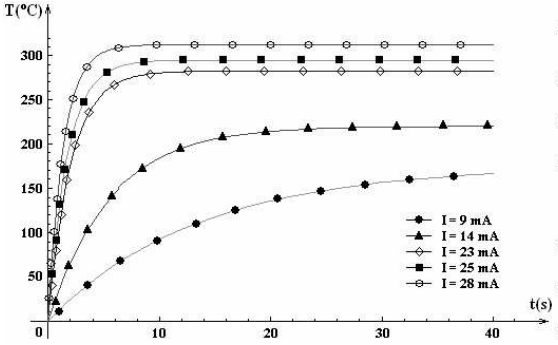

Fig. 5. The temporal evolution of the temperature $T(t)$ resistivity in center of the AGCM.

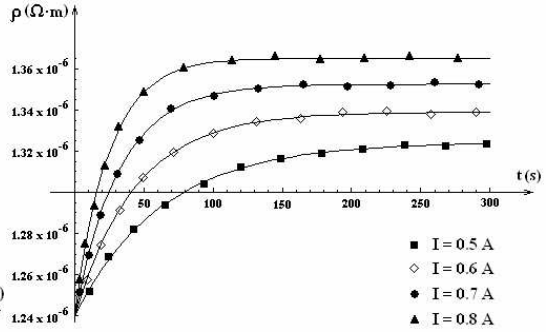

Fig. 6. The temporal evolution of the electrical center of the ribbon.

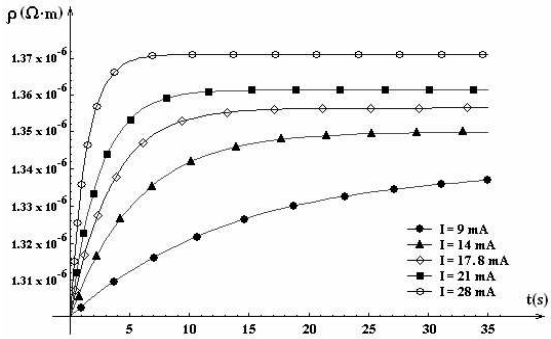

Fig. 7. The time evolution of the electrical resistivity in the center of the conventional wire.

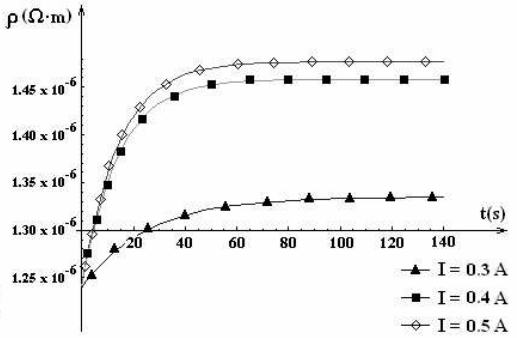

Fig. 8. The time evolution of the electrical resistivity for AGCM.

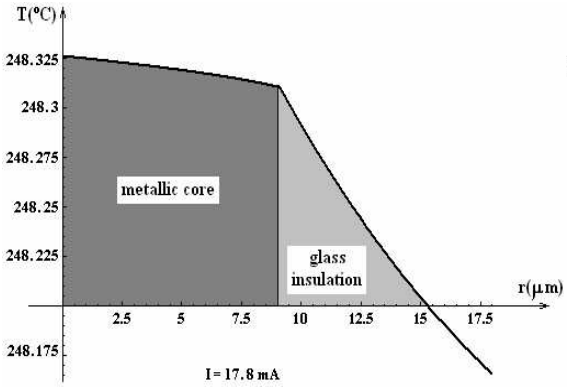

Fig. 9. The temperature distribution at the thermal equilibrium in the microwire's cross-section for a value of the d. c. $I = 17.8\ mA$.

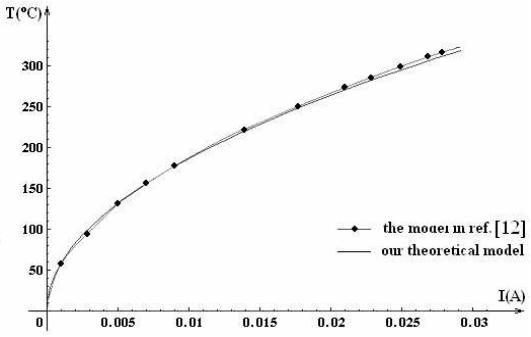

Fig. 10 The temperature as function of annealing current at the point $r = 1\ \mu m$ in the microwire's metallic core. The correlation between the two theoretical models is shown.

6. Conclusions

The above discussed improved theoretical model presents the thermal behavior of the amorphous magnetic materials (ribbons, conventional wires and glass-covered microwires) passed by an electrical d.c., taking into account the d.c. Joule heating effects (conduction, radiative and convection heat losses) and the structural changes appeared during the crystallization process.

As it is very well known, an electrical resistivity variation leads to a variation of the developed Joule power, and, subsequently, to a corresponding variation in the temperature distribution. For this reason, it is necessary to consider at least a linear dependence of the resistivity on temperature. Also, the thermal convective losses can not be neglected, whatever is the quality of the vacuum.

In the amorphous state of the above magnetic materials we have determined the temporal distributions of the temperature (Figs. 3, 4, 5) and temporal distributions of the electrical resistivity (Figs. 6, 7, 8). These results are very useful in order to improve the mechanical, magnetic and electrical properties of these amorphous magnetic materials.

For the ribbon, by analyzing the spatial distribution of the temperature at the thermal equilibrium (21), we have found that for different values of the electrical d.c., the equilibrium temperature is approximately constant in its thickness, but varies significantly in its width. This behavior can be explained by the numerical evaluations of the radiative and convection heat losses. The calculated values of the temperature for different values of the electrical d.c. are very close to those found by magnetic measurements of the Curie temperature.

For the conventional wire, the theoretical and experimental considerations are separately referring to the two different situations, namely:

1. for the amorphous state, when the temperature values are below the onset temperature of crystallization;
2. for the transition from the amorphous to the crystalline state, when both phases appear.

In the amorphous state, using the relation (34), we have analyzed the temperature distribution at the thermal equilibrium in the wire's cross-section for a value of the electrical d.c. $I = 0.1\,A$. It results that the temperature difference between the center of the wire and its surface is very small. Thus, it can be considered that the temperature is constant in the wire's cross section, the Joule heating ensuring in this way a uniform annealing of the wire.

Concerning the temperature domain situated above the temperature corresponding to the onset of the crystallization process, we have analyzed the thermal behavior and we have studied the crystallization phenomenon for the non-isothermal process (on the basis of the JMA equation). We have determined the temporal evolution of the temperature and the crystallized volume fraction as a function of time. In the non-isothermal crystallization process we have considered the Avrami crystallization rate parameter $K[T]$ to have an Arrhenius type temperature dependence, while the nucleation frequency K_0 was considered to be constant. The numerical analysis based on the Runge-Kutta-like method of 4-order for a system of two differential equations implemented in the specialized Mathematica 4.0 software allowed for getting the graphical dependencies for the temperature and electrical resistivity as a function of time. Thus, from DSC analysis (Fig. 2), we observe the two crystallization stages (two peaks) in the annealing of the conventional wire. The graphical representations in Figs. 1 and 2 clearly exhibit these crystallization stages of amorphous conventional wires in the non-isothermal crystallization process. Numericall results obtained for the Joule-heating treatment are in very good agreement with the experimental data obtained from DSC measuring method.

For the glass-covered microwire, we have found that, in comparison with the model proposed in [12], where the agreement with the experiment is ensured by best fit of the parameter $R(I)$, in the proposed theoretical model this agreement is provided by the self-consistency of the model.

References

[1] P. T. Squire, D. Atkinson, M. R. J. Gibbs, S. Atalay, J. Magn. Magn. Mater. **132**, 10 (1994).
[2] M. Vázquez, C. Gómez-Polo, D. X. Chen, A. Hernando, IEEE Trans. Magn. **30**, 907 (1994).
[3] P. Allia, M. Baricco, M. Knobel, P. Tiberto, F. Vinai, *Mat*. Sci. Eng. **A179/A180**, 361 (1994).
[4] P. Allia, M. Baricco, P. Tiberto, F. Vinai, Phys. Rev. **B 6**, 3118 (1993).
[5] P. Allia, M. Baricco, P. Tiberto, F. Vinai, Rev. Sci. Instr. **64**, 1053 (1993).
[6] C. Moron, C. Arocá, M.C. Sánchez, E. Lopez and P. Sánchez, IEEE Trans. Magn. **30**, 53 (1994).
[7] M. Knobel, P. Allia, C.Gómez-Polo, H. Chiriac, M. Vázquez, J.Phys. D: Appl.Phys. **28**, 2398 (1995).
[8] H. Chiriac, I. Astefanoaei, Phys. Stat. Sol. **A 153**, 183 (1996).
[9] P. J. Schneider, Conduction Heat Transfer, Addison Wesley Publishing Company Inc., 1955.
[10] J. W. Christian, The theory of Transformations in Metals and Alloys, Pergamon, Oxford, 1975.
[11] R. W. Cahn (editor), Physical Metallurgy, North-Holland Publishing Company, Amsterdam-New-York-Oxford, 1970, pp. 516.
[12] H. Chiriac, M. Knobel T.A. Óvári, Mat. Sci. For. 302-303 (1999).